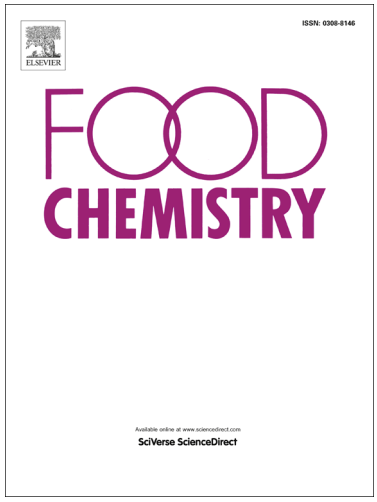

Temperature Dependent Raman and X-ray Diffraction studies of Anhydrous Milk Fat

A. Lambert, F. Bougrioua, O. Abbas, M. Courty, M. El Marssi, V. Faivre, S. Bresson

PII: S0308-8146(17)31457-7
DOI: http://dx.doi.org/10.1016/j.foodchem.2017.09.006
Reference: FOCH 21675

To appear in: *Food Chemistry*

Received Date: 5 March 2017
Revised Date: 6 July 2017
Accepted Date: 1 September 2017

Please cite this article as: Lambert, A., Bougrioua, F., Abbas, O., Courty, M., El Marssi, M., Faivre, V., Bresson, S., Temperature Dependent Raman and X-ray Diffraction studies of Anhydrous Milk Fat, *Food Chemistry* (2017), doi: http://dx.doi.org/10.1016/j.foodchem.2017.09.006

Temperature Dependent Raman and X-ray Diffraction studies of Anhydrous Milk Fat

A. Lambert[1*], F. Bougrioua[1], O. Abbas[2], M. Courty[3], M. El Marssi[4], V. Faivre[5], S. Bresson[1]

[1]*Laboratoire de Physique des Systèmes Complexes, Université Picardie Jules Verne, 33 rue S[t] Leu 80039 Amiens cedex, France*
[2]*Walloon Agricultural Research Centre (CRA-W), Valorisation of Agricultural Products, Department, Food and Feed Quality Unit (U15), 'Henseval Building', Chaussée de Namur 24, 5030 Gembloux, Belgium*
[3]*Laboratoire de Réactivité de Chimie du Solide, Université Picardie Jules Verne, 33 rue S[t] Leu 80039 Amiens cedex, France*
[4]*Laboratoire de Physique de la Matière Condensée, Université Picardie Jules Verne, 33 rue S[t] Leu 80039 Amiens cedex, France*
[5]*Institut Galien Paris-Sud, Univ. Paris-Sud, Université Paris-Saclay 5 rue JB Clément, 92296 Châtenay-Malabry, France*

ABSTRACT

Raman spectroscopy was used to characterize the polymorphs and liquid state of anhydrous milk fat, with emphasis placed on the thermal evolution of the ester carbonyl stretching modes (1800-1700 cm^{-1}) and the comparative study of the Raman-active C=C (1660 cm^{-1}) and C-H (3000-2700 cm^{-1}) vibrational modes. Specific Raman signatures in the crystalline phase were found and attributed to the coexistence of two groups of triglycerides. This was confirmed using differential scanning calorimetry and X-ray diffraction methods. In the ester carbonyl band, the effect of changing temperature on both the number of modes and new defined intensity ratios was studied and enabled polymorph discrimination. C-H stretching signals increased with polymorph stability, indicating the dominance of antisymmetric C-H methylene vibrations as the anhydrous milk fats crystal lattice became more ordered. The change in intensity of the C-H stretching bands as a function of temperature was used to probe the order-disorder transition.

KEYWORDS: Raman spectroscopy, Anhydrous Milk Fats, X-ray diffraction, liquid state, crystallization, polymorphism, DSC.

*corresponding author (albane.lambert@wanadoo.fr)

1. Introduction

Anhydrous milk fat (AMF) are mainly composed of triacylglycerols (98%), which are triesters of fatty acids and glycerol. According to Gresti (Gresti *et al.*, 1993), the composition of milk fats (MF) is complex and rich since they contain a large variety of fatty acids (more than 400) and triacylglycerol (TG) (more than 200). Partial replacement of cocoa butter with milk fat (MF) in chocolate formulations is today a standard industrial method, as it improves bloom resistance (Sonwai and Rousseau, 2010). Sonwai et al demonstrated that the presence of MF is beneficial to prevent fat bloom, but only beyond a critical concentration, meaning above 2.5% of the finished product.

Considering the variety of compounds in MF, their melting range are broad and spans from about -40°C to 40°C. In particular, Timms showed that TG could be separated into two groups: the short and the long chain length TG groups, which crystallize and melt at different temperatures (Timms, 1980). Thus, a complete study was carried out on our samples using differential scanning calorimetry. A comparison was made between the resulting thermal behaviors with the ones of previous studies (Lopez *et al*, 2001a, 2001b and 2005; Kaufmann, 2012).

X-ray scattering diffraction has been used to investigate the various polymorphic forms of AMF in our samples. This method was also used successfully in the quoted studies of Lopez et al (Lopez *et al*, 2001a, 2001b and 2005).

Raman spectroscopy is a non-destructive vibrational spectroscopy technique which gives meaningful information about the molecular conformation in solid and liquid TG phases. Some bands of Raman spectra are particularly interesting to investigate polymorphic structure of AMF. The bands in the spectral region 3200-2700 cm^{-1} correspond to ν(C-H) stretching modes. The ν(C=O) ester carbonyl stretching region appears at 1800-1700 cm^{-1}, and the ν(C=C) stretching region (olefinic band) near 1660 cm^{-1}. Stefanov *et al* proposed spectroscopy methods (infrared spectroscopy and Raman spectroscopy) for the analysis of the fatty acids (FAs) content in milk or milk fat (Stefanov *et al*, 2010). Raman spectroscopy was also applied to the examination of milk fat globules (Gallier, 2011) and of lipids (Czamara *et al*, 2014)

In this work, we present the Raman spectral characterization of the key polymorphic forms of AMF at different temperatures. X-Rays diffraction (XRD) and differential scanning calorimetry (DSC) are the two technics used to reinforce the Raman results. This study constitutes an essential stage in the understanding of the effects of milk fatty acids on chocolate bloom process.

2. Materials and Methods

2.1 Anhydrous Milk Fat (AMF)

Anhydrous Milk Fat (99.7% purity), was purchased from Parmalat (Toronto, Canada) and used without further purification.

2.2 X-ray diffraction (XRD)

XRD patterns were continuously recorded in transmission mode using quartz capillaries (1.5 mm diameter, W. Müller, Berlin, Germany) and the X-ray generator was a long line focus sealed tube [Enraf Nonius; Netherlands, Cu anode (Kα of 1.54 Å)] operating at a voltage of 40 kV and a current of 20 mA. Two gas-filled linear detectors (1024 channels each, filled with an argon-ethane mixture) allowed collecting the data. With the settings in place, scattering q vectors ranging from 0.08 to 0.52 $Å^{-1}$ and from 1.00 to 2.00 $Å^{-1}$ were evaluated. The scattering vector was defined as $q = 4\pi\sin(\theta)/\lambda$, where 2θ is the scattering angle. Thanks to this scattering vector, it was possible to calculate the distances via $q=2\pi/d$. Calibration of the detectors was carried out using the XRD pattern of the 2Lβ form of pure tristearin (4.61, 3.84 and 3.70 ± 0.01 Å and 44.97 ± 0.05 Å) and that of the silver behenate (58.38 ± 0.01 Å). Microcalix, a microcalorimeter specially designed for installation in an X-ray beam, served as a thermostated sample holder. Peak spectral decomposition was obtained using Origin 5.0 software (OriginLab Corporation, Northampton, MA, USA).

2.3 Differential scanning calorimetry (DSC)

The DSC experiments were carried out on a Netzsch DSC 204F1 heat flux differential calorimeter at a heating rate of 2°C/min and under a constant argon flow with 200 mL/min. Samples weighed, around 20 mg, were enclosed in aluminum sample pans covered with a pierced lid. An empty aluminium sample pan with a pierced lid was used as a reference. Three characteristic temperatures were collected in the thermograms: T_{onset}, T_{max} and T_{offset}, which

correspond respectively to the beginning, the maximum and the end of every measured thermal events.

2.4 FT-Raman spectroscopy

The measurements were carried out at the Walloon Agricultural Research Center (CRA-W), Belgium.

FT-RAMAN spectra were acquired using a Vertex 70-RAM II Bruker FT-RAMAN spectrometer. This instrument works with an Nd: YAG laser (yttrium aluminium garnet crystal doped with triply ionised neodymium) with an incident laser wavelength at 1064 nm (9398.5cm^{-1}). The RAM II spectrometer is equipped with a liquid-nitrogen cooled Ge detector. FT-RAMAN spectra [4000-45cm^{-1}] were collected with a resolution of 1 cm^{-1} by co-adding 128 scans for each spectrum at room temperature.

2.5 Micro Raman spectroscopy

Raman spectroscopy measurements were performed in a backscattering microconfiguration using the 514.5 nm wavelength from an Ar-ion laser focused on the sample surface and giving a 1 µm diameter spot. The power density was of the order of 20 kW/cm^2. Scattered light was analyzed using a Jobin Yvon T64000 spectrometer, equipped with a liquid nitrogen cooled CCD detector. The spectrometer provides a wave number resolution better than 3 cm^{-1}. Raman spectra were recorded with parallelly polarised incident and scattered light beams. The observed sample temperature fluctuations were smaller than ±0.01 °C. Spectral scans between 3100-800 cm^{-1} were performed using a 200 s scan time. The region between 1800-1700 cm^{-1} was scanned instead during 600 s to improve the peak fitting. The raman spectra related to the ester carbonyl, the C-H stretching and the C-C skeletal regions were fitted as per Bresson (Bresson *et al*, 2005).

3. Results and discussion

3.1 *Polymorphic discrimination*

To define the domains of stability of the polymorphic structures of AMF, the effects of temperature on the positions and intensities of X-rays peaks were studied in details.

Firstly, the AMF sample was heated to liquid state to erase its polymorphic history. Next, it was cooled from 60°C to -20°C at 2°C/min. The structural evolution with temperature of the

sample was acquired for both SAXS (Small Angle X-ray scattering, Figs. 1a et 1b) and WAXS (Wide Angle X-ray scattering, Figs. 1c et 1d) configurations.

Above 22°C, the sample remains completely liquid as no diffraction peak is observed. When cooling down below 22°C, several peaks grow up. It is known that each triglyceride found in anhydrous milk fats can exhibit several crystalline forms. Peaks at small angles corresponds to long *d*-spacings, reflecting the lamellar organization of triglycerides. Peaks at wide angles are assigned to short *d*-spacings, defining distances separating the chains. Four peaks corresponding to long spacings of 71 Å (q=0.088 $Å^{-1}$), 43 Å (q=0.146 $Å^{-1}$), 37 Å (q=0.170 $Å^{-1}$) and 24 Å (q=0.262 $Å^{-1}$) are observed at small angles as the sample is cooled down. According to the literature (Lopez *et al,* 2001a and 2001b; Lopez *et al,* 2005), the *d*-spacing value of 71 Å, measured at T = -8°C, corresponds to a crystalline form with a trilayered stacking (3L), while the value of 43 Å results from the formation of a bilayered structure (2L). The peak at 37 Å relates to the second order of the 3L structure labeled $3L_{002}$, while the larger and less intense peak at 24 Å may include the third order of the same lamellar structure labeled $3L_{003}$, or the second order of the 2L structure labeled $2L_{002}$. We note that our results are in good agreement with those obtained by Lopez (see Table 1). Fig. 1b exhibits the behavior of the different Bragg reflections with respect to temperature: the 2L structure (peak at 43 Å) grows from 22°C and the thicker trilayered structure (peaks at 71, 37, and 24 Å) initiates at 12°C. It can be noticed also that the latter appears at 12°C instead of 22°C. This suggests a more important TG contribution to the peak growth due to the 3L stacking ($3L_{003}$) than the 2L stacking ($2L_{002}$) one.

The wide angles XRD pattern at -8°C (Fig. 1c) presents a doublet peak, an intense one at 4.15 Å (q=1.51 $Å^{-1}$) and a weak one at 3.81 Å (q=1.65 $Å^{-1}$), and a shoulder at 4.25 Å (q=1.48 $Å^{-1}$). The most intense peak can be attributed to the crystallization of the alkyl chains in the weakly organized form, α, which corresponds to their hexagonal packing. The weaker peak at 3.81 Å with the shoulder at 4.25 Å relates to the orthorhombic β' lateral packing (Lopez *et al* 2001a and 2001b). The WAXS results versus temperature confirm the SAXS ones: the peaks corresponding to triglycerides β' form (at 3.81 and 4.25 Å) appears at 22°C and the peak corresponding to the triglycerides hexagonal packing, in α form (at 4.15 Å), exists for temperatures equal or less than 12°C.

Furthermore, in the crystalline phase at T= -8°C, the coexistence of two separate groups of triglycerides is noticed. The first group, in α form, is characterized by 3L stacking with peaks at 71 Å ($3L_{001}$), 37 Å ($3L_{002}$) and 24 Å ($3L_{003}$) in SAXS diffraction pattern and a unique peak at 4.15 Å (3L) in WAXS diffraction pattern. The second identified group has its alkyl chains

organized in β' form and characterized by a 2L crystalline structure with peaks in SAXS patterns at 43 Å ($2L_{001}$) and in WAXS patterns at 3.81 and 4.25 Å.

Finally, the sample has been reheated at 2°C/min from -20°C to 60°C, inducing structural evolution of anhydrous milk fat with temperature, for both SAXS (Figs. 2a et 2b) and WAXS (Figs. 2c et 2d) patterns. The 3L crystalline structure melts around 15°C as suggested by the disappearance of the peaks at 71 Å ($3L_{001}$), 37 Å ($3L_{002}$) and 24 Å ($3L_{003}$). As for triglycerides in β' form corresponding to the peak at 43 Å ($2L_{001}$), it melts above 40°C. The same conclusion can be drawn for the WAXS experiments, meaning the disappearance of the 3Lα structure at T = 15°C as well as the 2Lβ' structure at approximately 40°C.

3.2 *Differential scanning calorimetry*

Milk fat contains a large variety of fatty acids, so there is no true melting point. The melting range of the sample is broad and spans from about -40°C to 40°C. Therefore, a complete study of the sample thermal behavior has been carried out with differential scanning calorimetry.

AMF has first been heated to 60°C (liquid state) at 2°C/min. Next, it has been cooled from 60°C to -100°C at 2°C/min. In Fig. 3a, the DSC curve in the temperature range [-80°C, 40°C] shows clearly two main exothermic events. The first one has a T_{onset}=21.5°C with a T_{max}=18.6°C. A second sharp exothermic event starts at T_{onset}=12.7°C with a T_{max}=10.5°C. We can note that our results are in good agreement with those obtained by Lopez (Lopez *et al*, 2001b) (see Table 2 in supplementary material) who also observed a two steps crystallization in similar fat.

In a further step, the sample has been heated at 2°C/min from -100°C to 60°C. The results are presented in Fig. 3b in the temperature range [-50°C, 50°C]. Three well separated endotherms can be observed. The temperature at the maximum of the first endothermic event is T_{max}=3.9°C. A second sharp and well-defined event spans from about 5.6°C to 26.2°C with a top temperature at T_{max}=15.1°C. The last endotherm has a T_{max}=33.8°C and a T_{offset}=40°C. The results are compared with literature in Table 2 (in supplementary material).

Similar to XRD patterns, the DSC curve exhibits no peak above 22°C (Fig. 3a), the sample is then totally liquid. The first exothermic event occurs when the first diffracting peak is coming out. It can be assumed that it corresponds to the transition from liquid state to 2Lβ'

organization. As for the second exothermic event observed at about T=12°C, it may correspond to the appearance of the α form. This also is consistent with the XRD results.

So, the coexistence of the unstable α form of triglyceride and the stable β' one occurs at 12°C or below. Since the transition from a stable form to an unstable one is forbidden, the 3Lα organization can only originate from the liquid state. In summary, the polymorphic structures of anhydrous milk fat on cooling at 2°C/min are: $liquid \xrightarrow{22°C} 2L\beta'$ and $liquid \xrightarrow{12°C} 3L\alpha$.

Afterwards, the sample has been heated at 2°C/min from -10°C to 51°C. We note after X-rays analysis that the triglycerides in 3L crystalline structure transits to another phase at 15°C and the triglycerides in β' form melt above 40°C. In DSC data, three endothermic events have been observed at T= 3.9, 15.1 and 33.8°C respectively.

According to Lopez (Lopez *et al*, 2001a), the first endotherm can be attributed mainly to the melting of the unstable 3Lα form: this broad peak may correspond to the progressive α to β' transition, associated with the 3L to 2L transformation. Such a polymorphic transition is frequently observed for pure compounds (Lavigne *et al.*, 1993; Minato *et al.*, 1997; Ollivon and Perron, 1985). According to Timms (Timms, 1980), the endotherm at 15.1 °C may correspond to the melting of monounsaturated triglycerides or trisaturated TG with one short chain which passes from α form to β' form, while the next endotherms around T=33.8°C are attributed to the melting of the more stable β' form of trisaturated TG with longer chains. The polymorphic structures of anhydrous milk fat when heating can then be summarized as follow:

- for the trisaturated TG with short chains: $3L\alpha \xrightarrow{15°C} 2L\beta' \xrightarrow{40°C} liquid$
- for the trisaturated TG with long chains: $2L\beta' \xrightarrow{40°C} liquid$

The DSC and X-rays data analyses both confirm the coexistence in crystalline phase of the two groups of triglycerides as already described before: the *α* form group (3L stacking and trisaturated TG with short chains), and the β' form group (2L crystalline structure and trisaturated TG with long chains).

3.3 *Raman spectra*

The full range Raman spectra of AMF recorded either by FT-Raman spectrometer at λ_{laser} = 1064 nm or by Raman micro-spectrometer at λ_{laser} = 514 nm are shown in supplementary material (Fig. 6a). They have both been collected at room temperature. We note that the

Raman results do not depend on the laser incident wavelength. Every Raman spectrum exhibits several bands (supplementary material, Fig. 6b). The signals in the spectral region 3200-2700 cm^{-1} correspond to the ν(C-H) stretching modes. The ν(C=O) ester carbonyl stretching region appears at 1800-1700 cm^{-1}, and the ν(C=C) stretching region (olefinic band) near 1660 cm^{-1}. In this study, we have focused on the ν(C-H), ν(C=O) and ν(C=C) stretching regions. The assignations of all the studied modes are given in Table 3 in supplementary material.

3.3.1 C-H stretching region

Raman spectra of AMF in ν(C-H) stretching region (3000-2800 cm^{-1}) are presented for different temperatures both for cooling and heating experiments in Figs. 4a and 4c. The solid lines represent the components fitted by Lorentzian functions. The frequency values of the modes discussed below are obtained by Lorentzian functions fit. The error has been estimated at $\pm 0.5 cm^{-1}$.

The symmetrical and antisymmetrical stretching modes of CH bond in methylene are particularly interesting. The Raman shift values of these modes are compared to literature in Table 3 in supplementary material. Indeed, in Fig. 4a when AMF sample has been cooled at 2°C/min from 60°C to -20°C, we observe that the intensity of the antisymmetric vibration $\nu_{as}(CH_2)$ at 2885 cm^{-1} becomes more significant as compared with the one of the symmetric vibration $\nu_s(CH_2)$ at 2850 cm^{-1}. Bresson *et al* proposed the ratio $r = I[\nu_s(CH_2)]/I[\nu_{as}(CH_2)]$ (I_{2845}/I_{2880}) to determine which of the symmetric and antisymmetric chain-chain interactions predominates. They observed that this ratio tended to decrease as the cocoa butter crystal lattice became more ordered, and demonstrated that *r* was sensitive to the TG conformation (Bresson *et al*, 2011). Thirty-four years before, Gaber and Peticolas (1977) proposed a semi-quantitative parameter to measure the degree of lateral inter-chain order and localized intra-chain conformational order, defined as $S_{lateral}$:

$$S_{lateral} = [r(sample) - r(liq)]/[r(cryst.) - r(liq)] \quad (1)$$

Where $r = I_{2845}/I_{2880}$; *r(liq)* represents the residual intensity in the liquid; *r(cryst)* represents the intensity of an isolated all-*trans* chain. We deduce from Eq(1) that $S_{lateral} = 1$ defines ordered chains and $S_{lateral} = 0$ disordered ones (Gaber and Peticolas, 1977).

In the case of cooling measurements, we have chosen to use the ratio $r = I_{2850}/I_{2885}$ as well as the $S_{lateral}$ parameter to quantify the changes occurring during the liquid-to-crystal phase transition: then the conformationally-distorted alkyl chains tend to self-organize into a metastable crystal lattice. The $S_{lateral}$ definition developed for the heating process has been

adapted to the cooling one as follows: $S_{lateral}$ = [*r*(sample) – *r*(cryst.)]/[*r*(liq) - *r*(cryst.)]. Results for cooling process are plotted in Fig. 4b, together with the ones of DSC. At the beginning of the experiment the sample is totally liquid, giving an $S_{lateral}$ equal to 1. When the first exothermic event around 22°C occurs, $S_{lateral}$ starts to decrease: it may correspond to the transition from liquid state to 2Lβ' organization. Between 15°C and 12°C the first exothermic event is completed and the second one starts. In this temperature range, the $S_{lateral}$ decrease is suddenly accelerated. This phenomenon may correspond to the transition from liquid state to 3Lα triglycerides polymorphic forms.

Fig. 4c shows the AMF Raman spectra in the spectral region 3000-2800 cm^{-1} when heating from -25°C to 45°C at 2°C/min. We observe that the intensity of the antisymmetric vibration $\nu_{as}(CH_2)$ at 2885 cm^{-1} becomes less significant when temperature is increased as compared with the behaviour of the symmetric vibration $\nu_{as}(CH_2)$ at 2850 cm^{-1}. For the analysis of the heating process, we have chosen to use the $S_{lateral}$ parameter defined by Eq(1).

A sharp decrease of the $S_{lateral}$ curve as a function of temperature indicates a loss in crystalline order. Combining $S_{lateral}$ and DSC data analyses highlights the consistency of the results: it looks like the $S_{lateral}$ curve change in slope occurs when an endothermic event starts (Fig. 4d). Indeed, at the beginning of the heating process, the sample is crystallized, so the $S_{lateral}$ is equal to 1. The value of $S_{lateral}$ decreases a little bit with the first endothermic event, which has a low DSC intensity. A second well defined and intense endotherm starts at about 7°C and is accompanied by an $S_{lateral}$ which decreases more rapidly. It seems to correspond to the phase transition of the trisaturated TG with short chains: $3L\alpha \xrightarrow{15°C} 2L\beta' \xrightarrow{40°C} liquid$. Around 22°C, the end of the second endothermic event corresponds to another significant decrease of $S_{lateral}$. The last endothermic event starts at about 25°C which coincides with a new $S_{lateral}$ decrease. All these events can be attributed to the phase transition undergone by the trisaturated TG with long chains: $2L\beta' \xrightarrow{40°C} liquid$. Finally, according to the DSC results, the sample is totally liquid above 40°C, which is coherent with an $S_{lateral}$ value that stops decreasing. Thus, the observed abrupt changes in slope of $S_{lateral}$ fit well with the thermal events recorded by DSC and reflects fully the AMF phase polymorphic transitions.

3.3.2 Carbonyl stretching region and olefenic band

In this section, the ν(C=O) ester carbonyl stretching region (1800-1700 cm^{-1}) and the ν(C=C) stretching region (olefinic band, at 1660 cm^{-1}) results will be discussed. These regions of

Raman spectra have been collected at different temperatures and are plotted in Fig. 5a (cooling process at 2°C/min from 50°C to -20°C) and Fig. 5c (heating process at 2°C/min from -20°C to 60°C)

First, Fig. 5a, shows the growth of the C=O vibrational mode peak when the temperature is decreased. Starting from 14°C, it is transformed into a doublet with a shoulder. The number of adjusted components by Lorentzian functions varies: from 60°C to 14°C, we note two components for the ester carbonyl stretching mode at 1750 and 1743 cm^{-1}, whereas from 14°C to -20°C, three components have been observed at 1750, 1743 and 1730 cm^{-1}. For the ν(C=C) stretching region, no change is observed: the peak centered at 1655 cm^{-1} with a shoulder at 1675 cm^{-1} remains constant and independent of temperature. *Cis* and *trans* configurations in unsaturated fatty acids give C=C stretching bands in the regions 1665-1650 and 1680-1670 cm^{-1}, respectively (Gallier *et al*, 2011; Czamara *et al*, 2014).
For the polycrystalline phase at T= -8°C, we note the existence of a doublet with a shoulder for the C═O stretching mode corresponding to three geometries of the "knuckle" joint group O–C═O in the unit cell. In the isotropic liquid phase (T=50°C), we observe two components for the C═O stretching mode. In this phase, the intermolecular forces exerted to the molecules are weaker than in the polycrystalline phase. Previously, we have demonstrated the co-existence of two different groups of triglycerides in AMF: the TG with short chains and the TG with long chains. These two groups have two different configurations in their respective unit cell: α form for the first one and β' form for the second one. So, the two observed components for the C═O stretching mode in liquid phase at 1750 and 1743 cm^{-1} seem to correspond to the two configurations observed in liquid phase. These spectra confirm that the C═O stretching mode behavior is a good tool for studying conformational variations. Contrary to the C═O stretching mode, the stretching vibrations of C═C bonds do not seem to vary with the phase. The frequency values of the C═C stretching mode remain constant: 1675 and 1655 cm^{-1} in both phases.

In Fig. 5b, three selected intensity ratios are plotted versus temperature (temperature range from 50°C to -15°C). They correspond to the three observed peaks components of the ester carbonyl group when cooling down (see Fig 5.a) and defined as I_{1730}/I_{1743}, I_{1750}/I_{1743} and I_{1730}/I_{1750}. On the one hand, the mode at 1730 cm^{-1} appears only from 14°C, corresponding to the crystallization of the triglycerides with short chains. This could indicate that the

vibrational behavior of this mode is directly associated with the triglycerides of AMF in 3Lα organization in the crystalline phase. On the other hand, the intensity ratio I_{1730}/I_{1743} seems to be stable between T= 12°C and T= -15°C. This means these two modes have the same intensity behavior with temperature. From 22°C, we observe that I_{1750}/I_{1743} intensity ratio begins to fall from 1.15 to 0.60. Based on DSC and X-rays results, we know that the triglycerides with long chains change from liquid phase to 2Lβ' *o*rganization at T=22°C. This seems to indicate that the C=O mode at 1743 cm^{-1} increases when the triglycerides crystallize in *β'* form. From 12°C, the I_{1750}/I_{1743} ratio further decreases while triglycerides with short chains have just begun their crystallization into *α* form. This indicates that the vibrational behavior of the mode at 1743 cm^{-1} is associated with the contribution of the two TG groups at the same time. From 12°C, the intensity ratio I_{1730}/I_{1750} increases from 0.60 to 1.20: the contribution of the mode at 1730 cm^{-1} increases especially as the crystallization of triglycerides with short chains in α form stabilizes. Thus, according to the thermal behavior of the three studied intensity ratios in the ester carbonyl stretching region, the vibrational contributions of the two modes, one at 1750 cm^{-1} and the other at 1730 cm^{-1}, reflect the existence of triglycerides in β' form and in α form, respectively. The mode at 1743 cm^{-1} is instead connected at the same time to the vibrational contribution of both triglycerides groups.

When the sample is heated from -40°C to 50°C at 2°C/min (Fig. 5c), we observe the same phenomenon as under cooling, the passage from 3 to 2 components for the C=0 vibrational mode of ester group in isotropic liquid phase. Nevertheless, we note one difference: upon heating the DSC and X-rays results have shown that the TG with short chains evolve from a 3Lα organization to a 2Lβ' around 15°C, before changing into isotropic liquid phase around 40°C. In order to analyze these transitions, we have introduced in Fig. 5d the same three different intensity ratios between the three observed components of the ester carbonyl group as in Fig 5b. The three intensity ratios remain constant up to 0°C. Between 0°C and around 15°C, I_{1730}/I_{1750} increases from 0.90 to 1.10, whereas I_{1730}/I_{1743} and I_{1750}/I_{1743} fluctuate between 0.75 and 0.65, with a change around T = 5°C. From 15°C to 30°C, every intensity ratio evolves in a different way: I_{1730}/I_{1743} remains stable, I_{1750}/I_{1743} increases quickly from 0.60 to 0.90, whereas I_{1730}/I_{1750} decreases rapidly from 1.10 to 0.00. All these changes are in good agreement with our previously presented DSC and on X-rays results upon heating: for the trisaturated TG with short chains, we observe the successive transitions $3L\alpha \overset{15°C}{\rightarrow} 2L\beta' \overset{40°C}{\rightarrow} liquid$ and for the trisaturated TG with long chains $2L\beta' \overset{40°C}{\rightarrow} liquid$. Thus, in

the temperature range 10°C – 30°C, the decrease in I_{1730}/I_{1750} value can be understood as the reduction in intensity of the mode at 1730 cm^{-1} and the increase in intensity of the mode at 1750 cm^{-1}. This expresses the transformation of TG with short chains from the 3Lα organization to the 2Lβ' one. The sample is then a mixture of TG with short chains and long chains in β' form. The explanation for the I_{1730}/I_{1743} stability under cooling is identical to that obtained when heating: the two observed modes have the same intensity behavior in the considered temperature range.

Thus, the vibrational behavior of the ester stretching mode is a determining marker revealing any molecular configuration modification versus temperature within AMF structure.

Conclusion

In this work, we characterized the structural and vibrational changes of AMF as a function of temperature, for both cooling and heating experiments by X-ray diffraction, Differential Scanning Calorimetry and Raman spectroscopy.

The X-ray diffraction study showed that two different groups of triglycerides coexist in crystalline phase. TG from the first group are in α form. They are characterized by 3L lamellar organization at 71 Å ($3L_{001}$), 37 Å ($3L_{002}$) and 24 Å ($3L_{003}$) with SAXS diffraction pattern and a unique line at 4.15 Å (3L) with WAXS diffraction pattern. The second group of TG are organized in the more stable β' form and characterized by a 2L crystalline structure with lines in SAXS at 43 Å ($2L_{001}$) and in WAXS at 3.81 and 4.25 Å.

From these results in X-Ray diffraction, we have studied the thermal behavior of the sample. The consistency of the DSC results with X-Ray diffraction measurements led us to assume the following changes of polymorphic structures of anhydrous milk fat: $liquid \overset{22°C}{\rightarrow} 2L\beta'$ and $liquid \overset{12°C}{\rightarrow} 3L\alpha$. In the same way, heating experiments of anhydrous milk fat could then be summarized as follow for the trisaturated TG with short chains: $3L\alpha \overset{15°C}{\rightarrow} 2L\beta' \overset{40°C}{\rightarrow} liquid$ and for the trisaturated TG with long chains: $2L\beta' \overset{40°C}{\rightarrow} liquid$.

Raman spectroscopy experiments have been carried out on the AMF sample to study the ν(C-H) stretching modes (3200-2700 cm^{-1}), the ν(C=O) ester carbonyl stretching region (1800-

1700 cm^{-1}) and the ν(C=C) stretching region (olefinic band) near 1660 cm^{-1}. These spectral regions are important markers of the structural changes observed in XRD and DSC data. First, the changes in slope versus temperature of the semi-quantitative parameter $S_{lateral}$ seem to confirm the AMF phase polymorphic transitions measured by XRD and DSC. Then, the ester carbonyl region study permits to identify the existence of the two types of trisaturated TG due to the number of components. Indeed, the two observed components for the C=O stretching mode in liquid phase at 1750 cm^{-1} and 1743 cm^{-1} can be related to TG with short chains which are in α form at low temperature and to TG with long chains in β' form when the sample is crystallized. Further information can be provided by study of the ν(C=O) ester carbonyl stretching region. The changes in slope observed for the selected ratios I_{1730}/I_{1743}, I_{1750}/I_{1743} and I_{1730}/I_{1750} seems to be a new relevant tool to detect the above studied transformations. The olefinic band exhibits no evolution with temperature, so it can be assumed that the ν(C=C) stretching region is not affected by fat phase polymorphic transitions.

Acknowledgment

We would like to thank Quentin Arnould, technician of *Walloon Agricultural Research Centre (CRA-W)*, who participated to FT-Raman measurements.

References

Bresson S., El Marssi M. and Khelifa B. (2005). Raman spectroscopy investigation of various saturated monoacid triglycerides. *Chemistry and Physics of Lipids,* 134, Issue 2, 119-129

Bresson S. Rousseau D, Ghosh S, El Marssi M, Faivre V (2011). Raman spectroscopy of the polymorphic forms and liquid state of cocoa butter. *Eur. J. Lipid Sci. Technol.* 113 (8), 992-1004

Czamara K., Majzner K., Pacia M.Z., Kochan K., Kaczor A. and Baranska M. (2014). Raman spectroscopy of lipids: a review. *Journal of Raman Spectroscopy* (wileyonelinelibrary.com) DOI 10.1002/jrs4607

Gaber B.P. and Peticolas W.L. (1977). Quantitative interpretation of biomembrane structure by Raman spectroscopy. *Biochim. Biophys. Acta* 465, 260-274

Gallier S., Gordon K.C., Jiménez-Flores R., Everett D.W. (2011). Composition of bovine

milk fat globules by confocal Raman microscopy. International Dairy Journal 21, 402-412

Gresti J., M. Bugaut, C. Maniongui, and J. Bezard. (1993). Composition of molecular species of triacylglycerols in bovine milk fat. *J. Dairy Sci.* 76,1850–1869.

Kaufmann N., Andersen U., Wiking L. (2012). The effect of cooling rate and rapeseed oil addition on the melting behaviour, texture and microstructure of anhydrous milk fat. *International Dairy Journal* 25, 73-79

Lavigne F.C, Bourgaux . C., and Ollivon M. (1993). Phase transition of saturated triglycerides. *Suppl. J. Phys.* I. 3,137–140.

Lopez C, Lavigne F., Lesieur P., Bourgaux C. and Ollivon M. (2001a). Thermal and structural behavior of Milk Fat. 1. Unstable species of anhydrous milk fat. *J. Dairy Sci.* 84, 756-766

Lopez C, Lavigne F., Lesieur P., Keller G. and Ollivon M. (2001b). Thermal and structural behavior of Milk Fat. 2. Crystalline forms obtained by slow cooling. *J. Dairy Sci.* 84, 2402-2412

Lopez C, Lesieur P., Bourgaux C. and Ollivon M. (2005). Thermal and structural behavior of Milk Fat. 3. Influence of cooling rate. *J. Dairy Sci.* 88 (2), 511-526

Minato,A., S.Ueno,K. Smith, Y.Amemiya, and K. Sato. (1997). Thermodynamic and kinetic study on phase behavior of binary mixtures of POP and PPO forming molecular compound systems. *J. Phys. Chem.* 101, 3498–3505.

Ollivon, M., and R. Perron. (1985). Fat Science, Part A. *J. Hollo, ed. Elsevier*, New York, NY.

Sonwai S. and Rousseau D. (2010). Controlling fat bloom formation in chocolate – Impact of milk fat on microstructure and fat phase crystallization. *Food Chemistry* 119 (1), 286 - 297

Stefanov I., Baeten V., Abbas O., Colman E., Vlaeminck B., De Baets B. and Fievez V. (2010). Analysis of Milk Odd- and Branched-Chain Fatty Acids Using Fourier Transform (FT)-Raman Spectroscopy. *J. Agric. Food Chem.* 58, 10804–10811

Timms R. E. (1980). The phase behavior and polymorphism of milk fat, milk fat fractions and fully hardened milk fat. *Austr. J. Dairy Technol.* 35, 47–53.

Figures captions

Fig. 1. Evolution of the small (a), (b) and wide angles (c), (d) X-ray diffraction spacing of the main peaks of anhydrous milk fat during cooling at 2°C/min between 60°C and -20°C.

Fig. 2. Evolution of the small (a), (b) and wide angles (c), (d) X-ray diffraction spacing of the main peaks of anhydrous milk fat during heating at 2°C/min between -20°C and 60°C.

Fig. 3. Differential scanning calorimetry (DSC) recordings measured during cooling at 2°C/min between 60°C and -20°C (a), and heating at 2°C/min between -20°C and 60°C (b).

Fig. 4. The micro-Raman C-H stretching region (3000 - 2800 cm^{-1}) of AMF fitted by Lorentzian curves: spectra at 4 different temperatures when cooling at 2°C/min between 60°C and -20°C (a) and heating at 2°C/min between -20°C and 60°C (c). $S_{lateral}$ values of AMF as a function of temperature during cooling (b) and heating (d). The solid lines in (a) and (c) represent the components fitted by Lorentzian functions. DSC curve is superimposed to the $S_{lateral}$ one in (b) and (d).

Fig. 5. The micro-Raman carbonyl stretching region (1780 - 1700 cm^{-1}) fitted by Lorentzian curves of AMF: spectra at 4 different temperatures when cooling at 2°C/min between 60°C and -20°C (a) and when heating at 2°C/min between -20°C and 60°C (c). The solid lines represent the components fitted by Lorentzian functions. Raman intensity ratios I_{1730}/I_{1743}, I_{1750}/I_{1743} and I_{1730}/I_{1750} versus temperature when cooling (b) and heating (d).

Supplementary material: Fig. 6. Comparative study of micro-Raman spectra of AMF (wavelength λ_{laser} = 514 nm) and FT-Raman spectra of AMF (λ_{laser} = 1064 nm) (a); Raman spectrum of AMF with the assignations of the main vibrational modes (λ_{laser} = 1064 nm) (b).

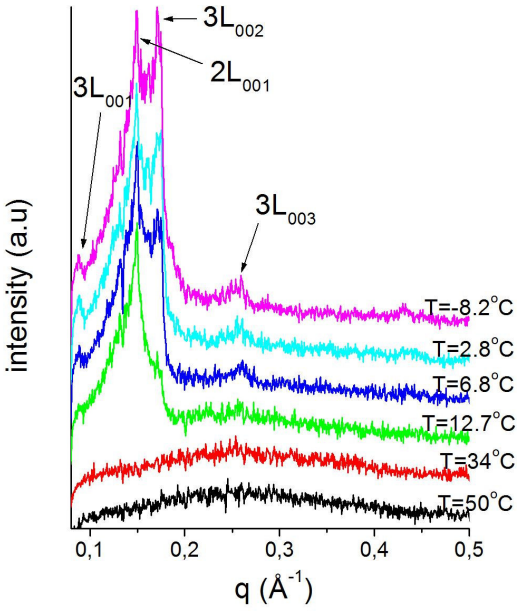

Fig. 1a

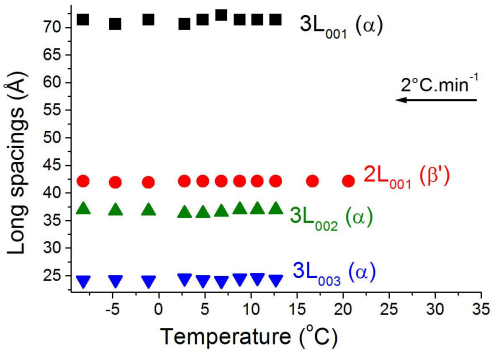

Fig. 1b

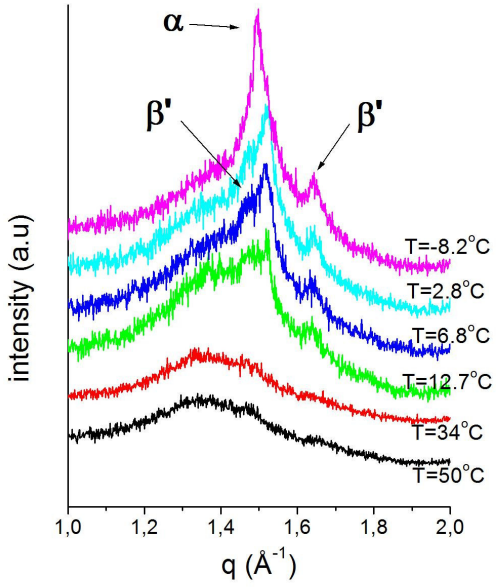

Fig. 1c

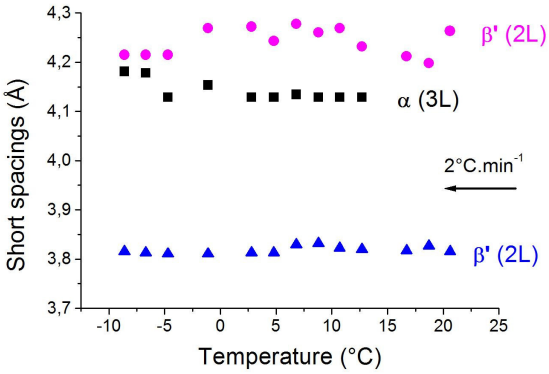

Fig. 1d

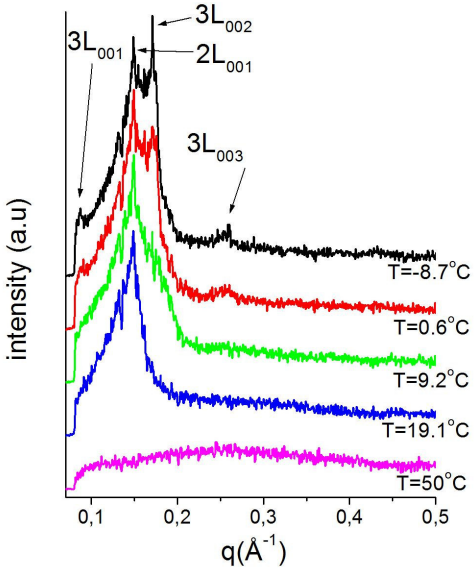

Fig. 2a

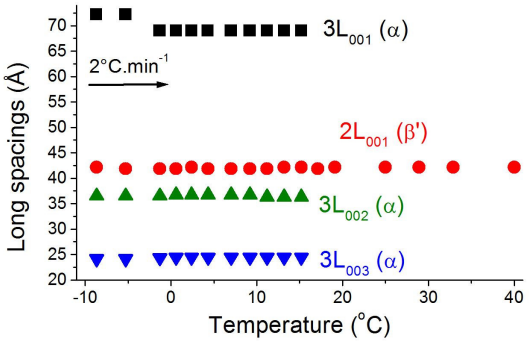

Fig. 2b

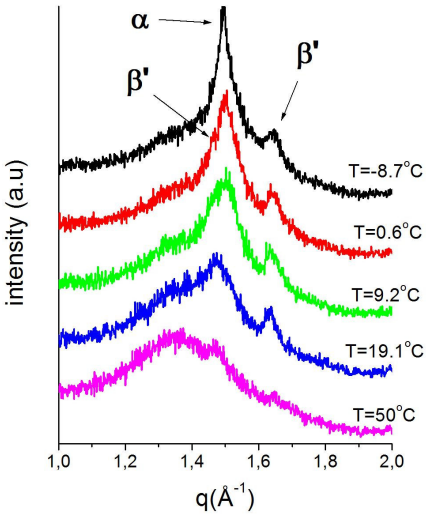

Fig. 2c

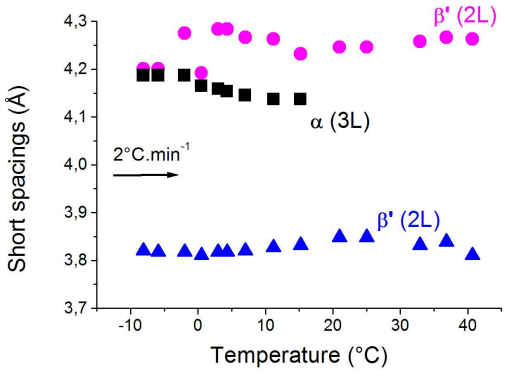

Fig. 2d

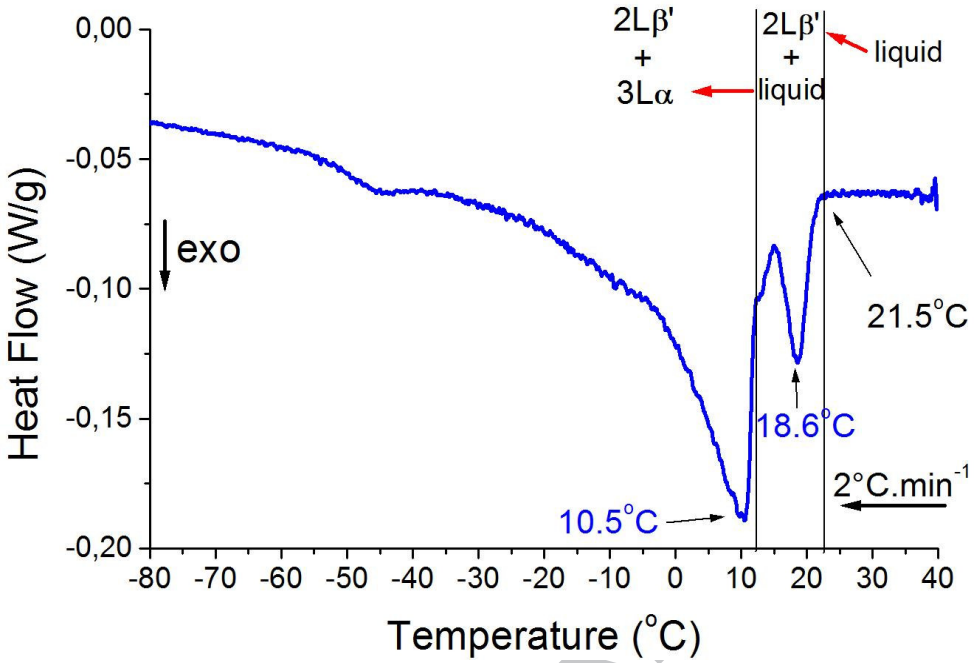
2Lβ'
+
3Lα
2Lβ'
+
liquid
liquid
exo
21.5°C
18.6°C
10.5°C
2°C.min-1
Heat Flow (W/g)
Temperature (°C)
0,00
-0,05
-0,10
-0,15
-0,20
-80 -70 -60 -50 -40 -30 -20 -10 0 10 20 30 40

Fig. 3a

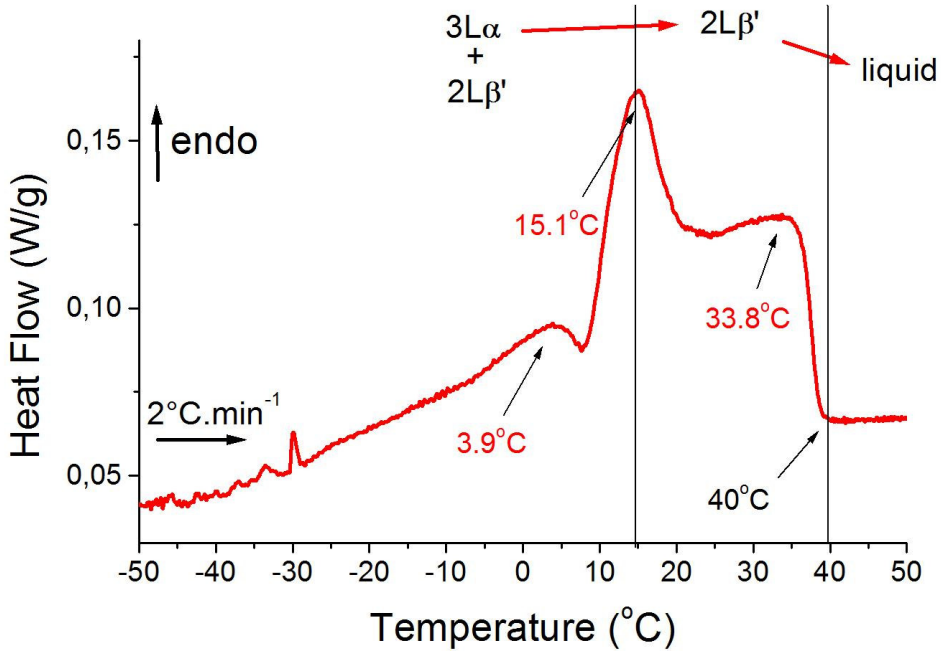
3Lα
+
2Lβ'
2Lβ'
liquid
endo
15.1°C
33.8°C
2°C.min-1
3.9°C
40°C
Heat Flow (W/g)
Temperature (°C)
0,15
0,10
0,05
-50 -40 -30 -20 -10 0 10 20 30 40 50

Fig. 3b

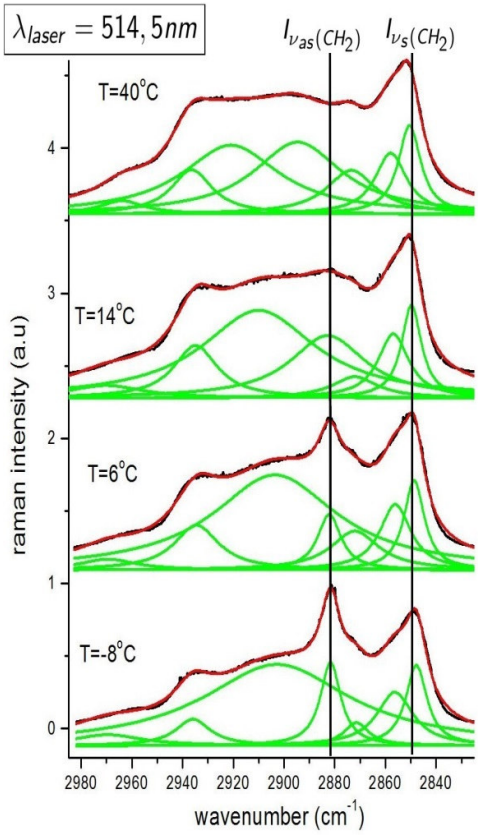

Fig. 4a

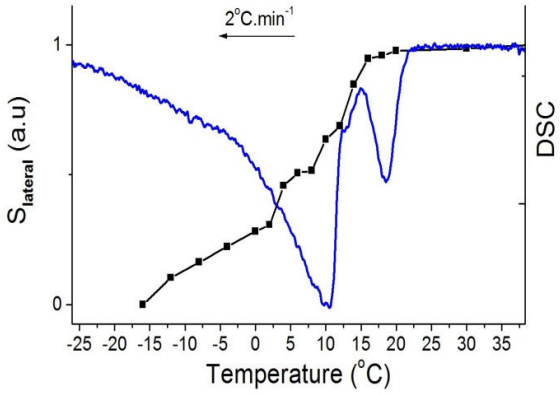

Fig. 4b

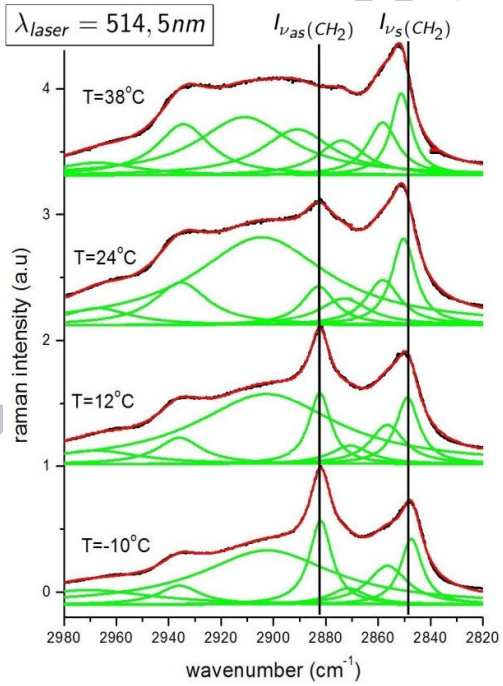

Fig. 4c

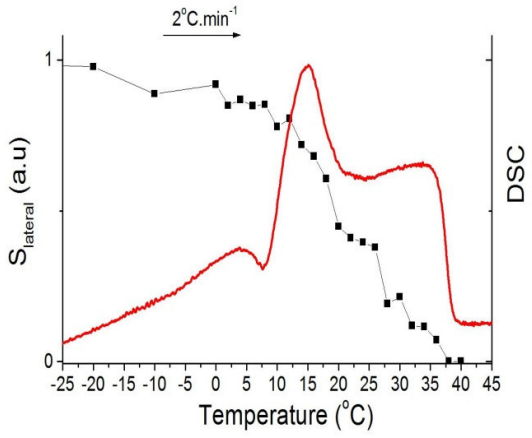

Fig. 4d

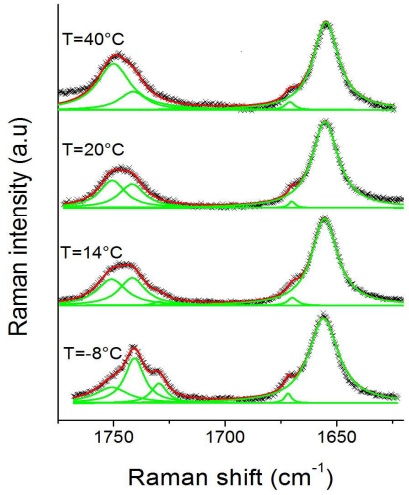

Fig. 5a

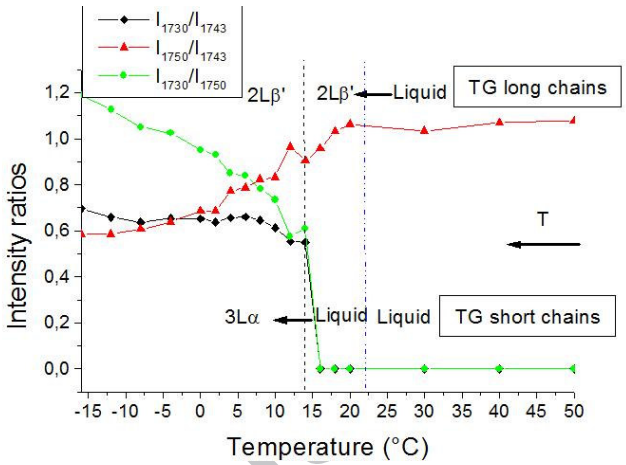

Fig. 5b

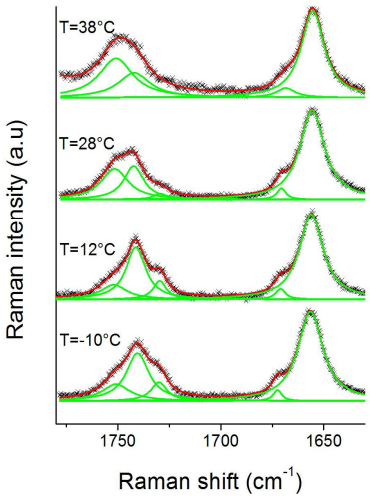

Fig. 5c

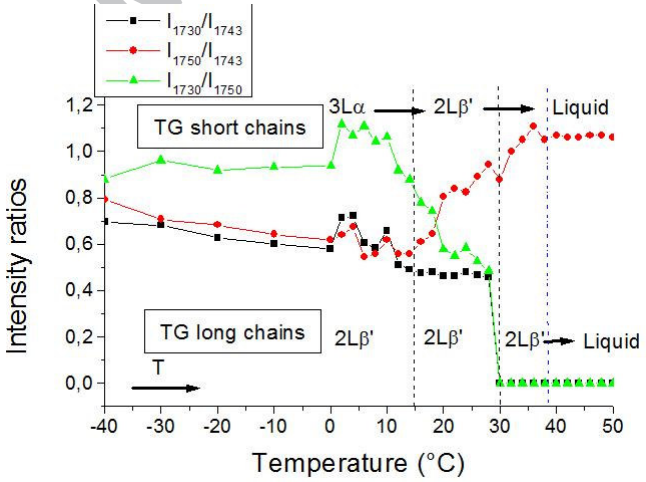

Fig. 5d

Table 1: Comparison of the crystalline parameters of the unstable forms of anhydrous milk fat. ([1] Lopez et al 2001b, [2] Lopez et al 2001a)

Crystalline organization	***Temperature in cooling***			***Temperature in heating***			
	22°C	**12°C**	**5°C**	**-8°C**	**3°C**	**17°C**	**22°C**
Long spacings and type ( )	43 Å (2Lβ') *42 Å (2Lβ')*[1]	71 Å (3Lα) 43 Å (2Lβ') 37 Å (3Lα) 24 Å (3Lα)	71 Å (3Lα) 43 Å (2Lβ') 37 Å (3Lα) 24 Å (3Lα)	74 Å (3Lα) 43 Å (2Lβ') 37 Å (3Lα) 24 Å (3Lα)	71 Å (3Lα) 43 Å (2Lβ') 37 Å (3Lα) 24 Å (3Lα) *70 Å (3Lα)*[2] *36 Å (3Lα)*[2] *24 Å (3Lα)*[2]	43 Å (2Lβ') *39 Å (2Lβ')*[2]	43 Å (2Lβ') *40 Å (2Lβ')*[2]
Short spacings and type ( )	4.25 Å (2Lβ') 3.81 Å *4.3 Å (2Lβ')*[1] *3.88 Å*	4.25 Å (2Lβ') 4.15 Å (3Lα) 3.81 Å (2Lβ')	4.25 Å (2Lβ') 4.15 Å (3Lα) 3.81 Å (2Lβ')	4.22 Å (2Lβ') 4.18 Å (3Lα) 3.81 Å (2Lβ') *4.22 Å (3Lα)*[2]	4.25 Å (2Lβ') 4.15 Å (3Lα) 3.81 Å (2Lβ') *4.19 Å (3Lα)*[2]	4.25 Å (2Lβ') 3.81 Å (2Lβ') *4.29 Å* (2Lβ')[2] *3.89 Å* (2Lβ')[2]	4.25 Å (2Lβ') 3.81 Å (2Lβ') *4.32 Å* (2Lβ')[2] *3.89 Å* (2Lβ')[2]

Highlights

- DSC and X-ray analysis: coexistence of two polymorphic groups of triglycerides
- Vibrational behavior of AMF in the spectral ranges 3000 – 2800 and 1800-1000 cm^{-1} according to the temperature
- In Raman spectra, C-H and C=O stretching modes are very sensitive to environmental changes
- Raman spectroscopy, DSC and X-ray are very complementary experiments